Segmented Polyurethane from Soyoil Polyols[*]

Ling Zhang [a], Hyun K. Jeon [a], Jeff Malsam [b], Ron Herrington [c], Christopher W. Macosko [a]

a) *Department of Chemical Engineering and Material Science*
University of Minnesota, 421 Washington Avenue SE., Minneapolis, MN 55455
b) *Process Solutions Technology Development Center, Cargill Inc.*
2301 Crosby Road, Wayzata, MN 55391
c) *Ron Herrington Consultancy*
2919 Country Road 510, Brazoria, TX 77422

Abstract

In this study three polyurethane (PU) flexible foams were prepared by using polyether polyol and by replacing 30% of the polyether polyol with soybean oil-derived polyol (SBOP) and styrene acrylonitrile (SAN) copolymer filled polyol. Scanning electron microscope, dynamic mechanical analysis (DMA), and small angle X-ray scattering (SAXS) were used to examine the cellular structure and the polymer morphology. Compared to the all petroleum-based PU foams, DMA of the SBOP-containing foam showed broader glass transition temperature accompanied by a more gradual decay of the storage modulus (G') with temperature. The SAXS results exhibited a decrease in signal intensity as SBOP is incorporated into the foam, which corresponds to a decrease in electron density contrast between the hard and soft phases. Both behaviors observed in DMA and SAXS suggest an increased degree of phase mixing in SBOP-containing foam.

Introduction

Polyurethane (PU) is one of the most versatile polymeric materials. It is widely used in construction, furniture, and transportation [1, 2]. PU is formed via reaction between hydroxyl-containing polyol and isocyanate, both of which are petroleum derivatives. The stability and the sustainability of the petroleum market are growing concerns, making development of alternative feedstock to PU production highly desirable [3].

Bio-based materials, such as vegetable oils, are potential candidates as precursors for polyol synthesis [4, 5]. They are considerably inexpensive, readily available, and not subject to a long life cycle as petroleum derivatives [6]. However, vegetable oils, with the exception of castor oil, do not bear hydroxyls naturally. Methods, such as hydroformylation followed by hydrogenation [5]; epoxidation followed by ring opening [4]; and ozonolysis followed by hydrogenation [7] are used to add hydroxyl groups at unsaturated sites.

Recently Herrington and Malsam [8] have successfully prepared flexible PU foam by substituting up to 30 wt% of the total polyol with SBOP. Startlingly, they observed significant loadbearing (LB) capability improvement in these substituted foams. LB capability is a measure of foam hardness and is tested using compression and/or deflection tests. In the published work by Herrington et. al., the LB was measured using ASTM D-3574 test B1 and results were reported as compression strength at 65% deformation.

---

[*] This paper has been submitted and accepted by SPE Foams 2006 Conference in Chicago IL.

The use of SBOP in PU flexible foam can potentially shift away the PU industry's dependence from petroleum. As an added benefit, it also provides an alternative to fine-tune foam compression strength/hardness, which is critical to manufactures. Foam hardness desired changes considerably based upon application. Existing methods for adjusting hardness involve (1) controlling foam density, (2) changing isocyanate index, (3) varying polyol functionality, and (4) addition of copolymer polyol. In the case of using SBOP to control foam hardness, improvement is achieved without involving any of the techniques. Compared to the use of copolymer polyol, a preferred method in industrial practice, SBOP production does not involve particle size control.

This work seeks to understand the basis for the improved compression strength observed by Herrington and Malsam. Anchoring the objective, three PU flexible foams were prepared by using polyether polyol and by replacing 30% of the polyether polyol with SBOP and styrene-acrylonitrile (SAN) copolymer-filled polyol. Scanning electron microscopy (SEM) images were used to study foam cellular structures and the analysis shows that cell size is slightly affected by substituent polyol. Small angle x-ray scattering (SAXS) and dynamic mechanical analysis (DMA) experiments were used to probe foam morphology. The SAXS results show an electron density contrast reduction in SBOP-containing foam but increase in SAN-containing foam. DMA test on SBOP-containing foam shows much gradual decay of storage modulus (G') with respect to temperatures and less sharp peak of tanδ at soft phase T_g. Both SAXS and DMA results concur that SBOP-containing foam is more phase mixed than those made with petroleum-based polyols.

<div align="center">Experimental</div>

Materials

Hyperlite[®] E848 (Bayer Corporation), was used as the base polyol. Hyperlite[®] E848 is a propylene oxide-based, ethylene oxide-capped polyol with a number average molecular weight (Mn) of 6703 g/mol and a functionality (fn) of 3.8. Hyperlite[®] E849 (Bayer Corporation) is a poly(styrene acrylonitrile) copolymer-filled polyol, containing 41 wt% stabilized SAN particles that are less than 1 μm in size. The Mn of Hyperlite[®] E849 is 11800 g/mol, and its fn is 3.8.

SBOP was synthesized by expoxidation of soybean oil followed by ring opening with a mixture of water and methanol, detailed procedures are available in reference 8. The Mn of SBOP is 1060 g/mol and fn is 3.8. An ideal structure is shown in Figure 1.
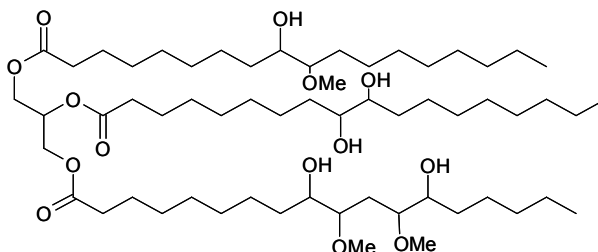
Figure 1. Idealized structure of SBOP used in this study

Toluene isocyanate (TDI) used is an 80/20 mixture of 2,4 and 2,6 isomers (Grade A Mondur[®] T-80, Bayer). Distilled water was used as only blowing agent. Gelling and

blowing catalysts, Dabco® 33LV and Dabco® BL11, were obtained from Air Products. Dabco® 33-LV is a solution of 33 wt% triethylene diamine in dipropylene glycol. Dabco® BL-11 is a solution of 70 wt% bis (2-dimethylaminoethyl) ether in dipropylene glycol. Diethanolamine (DEOA, Huntsman) was used as a foam stabilizer.

Three surfactants: Niax® Y-10184, Dabco® DC-5169, and Tegostab® B-4690 were used. Dabco® DC-5169 (Air Products) and Tegostab® B-4690 (Degussa AG) were used with a weight ratio of 1:3 in SBOP foam. Niax® Y-10184 (GE Silicon-OSI Specialties Inc.) is a silicon-based surfactant and was used in the foams not containing SBOP.

Foam Synthesis

All foams were made based on 100 parts total polyol and a total weight of 500 grams, formulation details are in Table 1. The stoichiometrically balanced amounts of TDI were used.

Table 1. Flexible foam formulation by weight and physical properties

Component	control	30% SAN	30% SBOP
Hyperlite® E848	100	70	70
Hyperlite® E849		30	
SBOP			30
Surfactant *	1.0	1.0	2.0
Dabco® 33-LV	0.16	0.16	0.16
Dabco® BL-11	0.08	0.08	0.08
DEOA	1.2	1.2	1.2
Water	4.2	4.2	4.2
TDI weight (g, index = 100)	156.7	155.3	172.2
Foam Density (kg/m^3)	32	32	32
65% IFD (N/323 cm^2)	260	357	600
G' at 25 °C (10^{-3}Pa)	10.5	17.7	51.8

*A mixture of Dabco® DC-5169 and Tegstab® B-4690 at 1:3 by weight was used in 30% SBOP foam; Niax® Y-10184 was used for others.

All ingredients, except TDI, were weighed and mixed in a 33-ounce paper cup at 1100 RPM for 24 seconds. Then pre-measured isocyanate was added and mixed for an additional 6 seconds. Mixture was transferred into an aluminum mold (38.1 cm x 38.1 cm x 11.4 cm) controlled at 66 °C ± 1 °C and cured for six minutes.

For each foam, the hard and soft segment contents were calculated. Hard segment (HS) includes TDI, water, hydroxyl from polyol, and excludes carbon dioxide released. Soft segment (SS) includes polyol except the hydroxyls. The HS concentrations and hard to soft segment ratios are shown in Table 2.

Table 2. Calculated HS weight percentages and hard to soft segment ratios.

Foam Sample	HS (%)	HS/SS ratio
control	28.1	28.1 : 63.6 = 0.442
30% SAN	27.7	27.7 : 55.7 = 0.497
30% SBOP	32.3	32.3 : 59.2 = 0.545

Solvent Extraction

A set of 6 samples were cut from the center of foam buns, dried at 60 ºC for 24 hours and weighed (0.1 to 0.2 grams). Each sample was subsequently immersed in 20 ml dimethyl formamide for 7 days at room temperature followed by drying in a vacuum oven at 60 ºC for 10 days. The weight losses were averaged.

Scanning Electron Microscope (SEM)

Foam was dipped in liquid nitrogen and cut with razor blade to rectangular slices: 7 x 10 x 2 mm. The slices were sputter coated with 50Å grain-sized platinum. Cellular structure was imaged with a field-emission gun scanning electron microscope (JEOL JSM-6500) operated at 5 keV. A total of 6-8 images were collected on each sample. Cell size was calculated by manually tracing the cell perimeter from the micrographs using ImageTool software and approximated the cells to circular shapes [9, 10]. An average of forty cells were used for analysis.

Dynamic Mechanical Analysis (DMA)

Circular discs of foam (25mm (D) x 10mm) were tested in a rotational rheometer (ARES II, TA Instrument) under oscillatory mode. The sample was secured between two 25 mm diameter, serrated parallel plates. A constant normal force of 50 g was applied throughout testing. Storage modulus (G′) was recorded (frequency = 1 Hz) as temperature ramped from −100 ºC to 250 ºC at 3 ºC/min. Two strains were used: 0.2% for temperature above 25 °C and 0.1% for temperature below. Both strains are within the linear viscoelastic region of foams in the corresponding temperature range.

Small Angle X-ray Scattering (SAXS)

Degree of phase separation in polymer phase was probed using SAXS. The SAXS setup is comprised of a Rigaku rotating anode with Cu source and a Siemens Hi-Star multi-wire area detector. The x-ray generator operates at 12kW and 40 mA. The

attainable scattering angle (θ/2) ranges from 0.18 to 38 degrees. About 10 mg of the foam sample was loaded inside a copper sample holder. Foam was then exposed to x-rays for 5 min. All raw data were corrected for parasitic scattering and normalized for sample thickness variation.

Differential Scanning Calorimetry (DSC)
    The glass transition temperatures of foams were determined using a DSC (Q1000, TA Instruments). 6-10 mg of a foam sample was sealed into an aluminum pan. The sample was first heated to 120 °C and held isotherm for 2 minutes, followed by cooling to -100 ºC and heated to 200 ºC at 10 ºC/min. Glass transition temperatures were determined as the second order transition of the exotherm curves.

Results and Discussion

The LB capacity of molded polyurethane flexible foams were measured using 65% indentation force deflection (IFD) test: method ASTM D 3574-95, test B1 and the results are in Figure 2. Both substituted foams showed LB improvement over control: 37% for the 30% SAN foam and a remarkable 131% for the 30% SBOP. The goal of this study is to provide an explanation for the LB improvement.
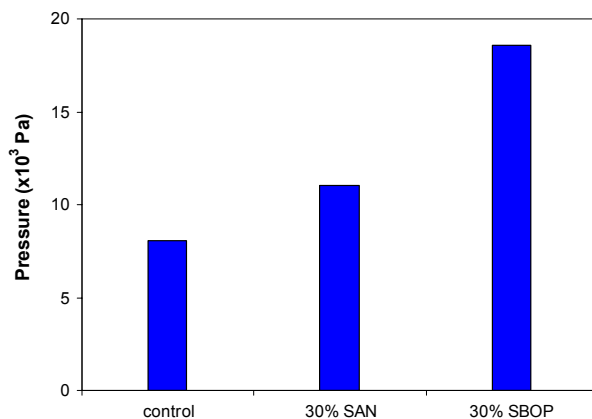
Figure 2. 65% IFD test results

Solvent Extraction
    The extraction experiments were used to evaluate network connectivity (Table 3). There is less than 2% extractable for both control and 30% SBOP foams. The lower sol fraction correlates to higher conversion of reactants. In this case, both base polyol and SBOP are covalently bonded into the polymer network. The noteworthy fact is that the secondary hydroxyls in SBOP are well reacted into the network as well.

Table 3. Sol fractions: the standard deviations of 6 samples per foam.

Sample Foam	Sol Fraction (%)
Control	1.31 ± 0.20
30% SAN	4.75 ± 0.37
30% SBOP	1.38 ± 0.18

The highest extractable is found in 30% SAN foam. Likely, extraction of SAN copolymer particles accounts for this higher sol fraction. Since SAN copolymers are surface-modified particles, which are not necessarily reactive, thus may not covalently bond to the polymer phase [11]. In spite of this, the total content of SAN copolymer in the 30% SAN foam is approximately 8 wt%, higher than the extractable fraction. Discrepancy between the extractable and total SAN content may due to physical trapping of large SAN particles.

Foam Cellular Structures

At equal foam density, cell size and polymer modulus control compression properties of foam [12-14]. Scanning electron micrographs were taken on foams to determine whether changes in compression modulus are related to the cell size changes. As Figure 3 and 4 show that substitutions of SAN copolymer polyol, and SBOP decrease cell size and broaden size distribution. Visually, the population of open cells is, nonetheless, similar in all (Figure 3).

Figure 3. SEM images: **(a)** control;**(b)** 30% SAN; and **(c)** 30% SBOP

SAN copolymer-filled polyol is effective in reducing cell size because SAN particles serve as additional nucleation sites for bubble growth [15]. Niederoest et. al. have demonstrated by replacing up to 70% of the total polyol with SAN filled polyol, cell size can be reduced from over 1mm to less than 0.1 mm in diameter [16].
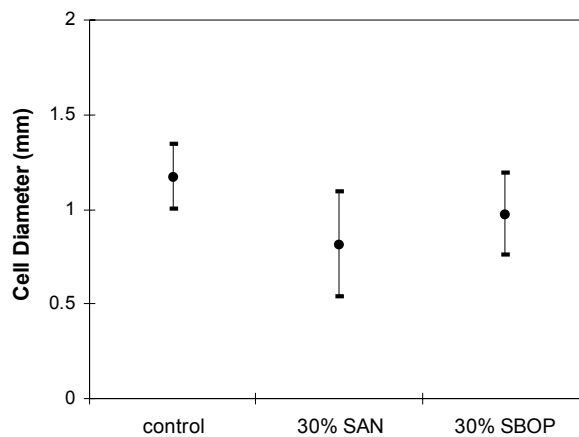
Figure 4. Average cell size and cell size distribution.

The 30% SBOP foam shows a minor cell size reduction, which may be due to the presence of dangling chains. These hydrocarbon chains can stabilize CO_2 bubbles and slow down coarsening.

Comparing average cell size data to the 65% IFD results, there is no apparent correlation. Therefore, polymer phase modulus plays the primary role in improving IFD, and, indeed, such correlation is observed between foam modulus at 25 ºC and their IFD.

Dynamic Mechanical Analysis (DMA)

DMA tests reveal substantial variations in modulus as the substituent polyol changes. When 30% of the polyether polyol is replaced by SAN filled copolymer polyol (Figure 5b), modulus G′ increases by approximately 60% from T_g (-65 °C) to 113 °C. This increase is a result of reinforcement via copolymers, because as temperature reaches beyond 113 °C, the modulus of 30% SAN foam falls to approximately the same level as control. The relaxation at 113 °C corresponds to the T_g of SAN copolymer.
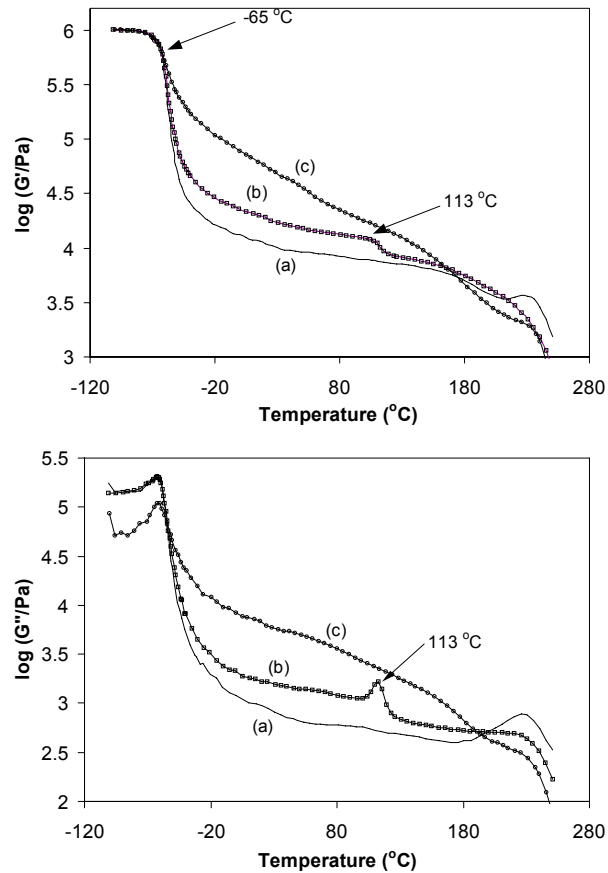
Figure 5. DMA results: **(a)** control; **(b)** 30% SAN and **(c)** 30% SBOP

The G′ data for the 30% SBOP foam is drastically different from either control or the 30% SAN. The curve (Figure 5, curve c) shows a small drop of G′ at T_g followed by a much gradual decrease of G′ over the temperature range. The small drop of G′ at T_g implies that only a small amount of the SSs are mobile at -65 °C, and as temperature increases, the population of mobile SS increases gradually. This behavior of G′ suggests

that 30% SBOP SS might be mixed with HS. In Figure 6, the tanδ versus temperature plot, a less sharp peak for 30% SBOP foam also suggests phase mixing.
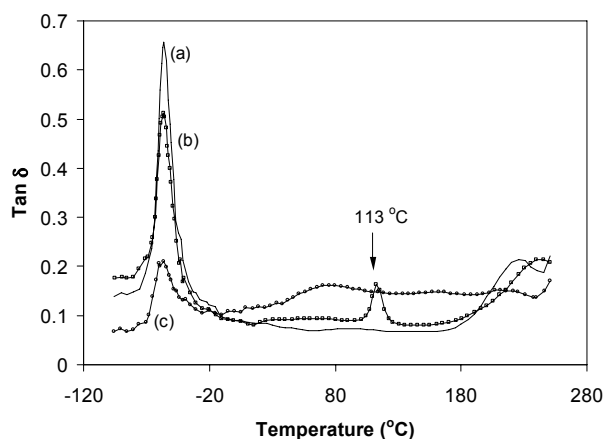
Figure 6. tanδ vs. temperature: **(a)** control; **(b)** 30% SAN and **(c)** 30% SBOP

Additionally, no rubbery plateau is observed in G′ curve of the 30% SBOP foam, which means hard domains in the foam are structurally irregular. Previous studies on poly(urethane-urea) gel networks found both rubbery plateau modulus and hard domain dissolution temperature, the temperature at which hydrogen bonding in hard domains breaks down, increase with increasing HS concentration [17-20]. In the case of 30% SBOP foam, its HS content is higher than the control (Table 2), and yet, the dissociation temperature is lower. This supports the previous hypothesis that HSs are mixed with SSs, because disrupted hard domains will result in lower dissociation temperature.

Small Angle X-ray Scattering (SAXS)
The SAXS results of foams show the characteristic broad peaks due to hard domain spacing distribution (Figure 7). The centers correspond to approximately 115 Å in domain spacing. A notable difference between samples is the signal intensity. Generally speaking, the SAXS signal intensity is controlled by two factors: (1) the volumetric ratio of hard domains (high electron density phase) to soft domains (low electron density phase) [21] and (2) the inherit electron density contrast between hard and soft domains. Factor (1) is associated with weight ratio of HS to SS in this case.
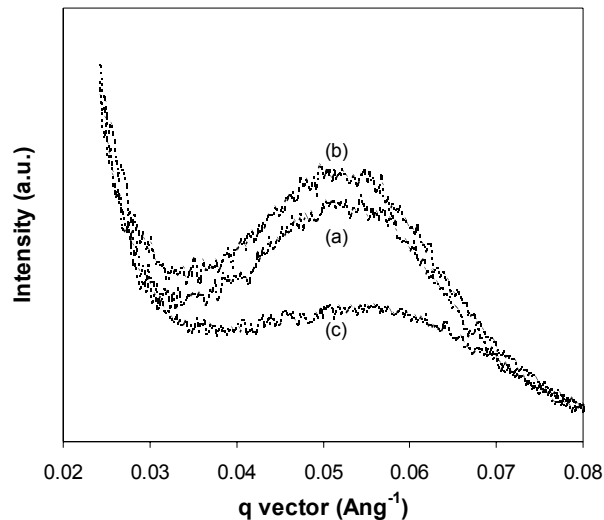
Figure 7. SAXS results: **(a)** control, **(b)** 30% SAN, and **(c)** 30% SBOP

The 30% SAN shows a higher intensity than the control, which is expected due to increased HS/SS ratio in sample. The 30% SBOP foam shows a much reduced signal intensity and is not anticipated. The SBOP is a triglyceride-based polyol, which is comprised of fatty acid chains. Compared to polyether SS, SBOP foam' SS is lower in electron density. With higher HS/SS ratio, higher electron density contrast is expected. The greatly reduced x-ray intensity in 30% SBOP foam is probably caused by a phase mixed morphology.

Differential Scanning Calorimetry (DSC)

All foams have similar SS glass transition temperatures (Figure 8) and are predominately that of the Hyperlite® E848 soft domain. The breadths of the T_g's, as well as ΔCp, are different. The onset and end of a transition is defined as the intersection of the neighboring two tangential lines of the heating curve (insert in Figure 8).
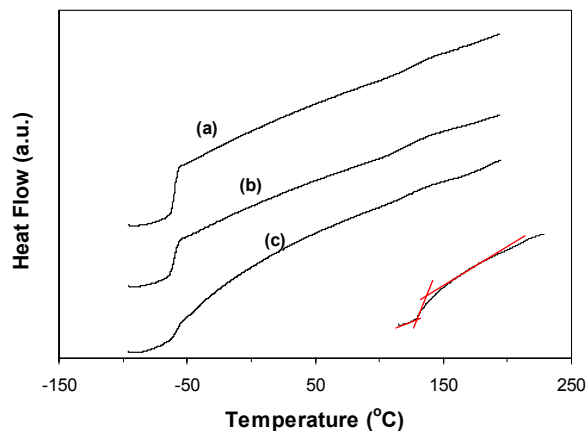
Figure 8. DSC results: **(a)** control, **(b)** 30% SAN, and **(c)** 30% SBOP. Insert illustrates the method used to determine ΔCp and breadth of T_g

The breadth of T_g increases as impurity in soft domain increases. The 30% SAN sample has a slightly larger breadth than the control. Both SAN copolymer and surfactants are likely the impurity in soft domains.

Table 4. Heat capacity change at T_g

Sample Foam	ΔCp (J/g/^{o}C)
Control	0.33
30% SAN	0.25
30% SBOP	0.16

The broadest T_g occurred in the 30% SBOP foam, where the tansition is hardly visible. Heat capacity changes over glass transitions were also determined in Table 4. Theoretically, the change in heat capacity at T_g scales with the weight percentage of free SS in foams. The ΔCp in 30% SBOP foam is 42% of that in the control whereas Hyperlite[®] E848 comprises 70% of total polyol in this foam. This means slightly more than half of the Hyperlite[®] E848 SS were mobile at T_g. Phase mixing between the SS and HS can certainly cause such behavior. When SS is mixed with HS, its mobility is restrained by the mobility of the HS. Thus, SS remains immobile even at temperature above its T_g. Additionally, no other T_g is detected on the 30% SBOP foam. It is rational to believe that SBOP is well mixed with Hyperlite[®] E848 polyol and hard segments.

Conclusion

This study focused on understanding the basis for improved compression strength in SBOP-containing PU flexible foam. A comparative study was conducted on foams made with 100% polyether polyol and by replacing 30% of the total polyol with SBOP and SAN copolymer-filled polyol.

The SEM micrographs analysis and modulus results show that although cell size reduction is observed as substituent polyols were added the compression modulus, however, is predominately determined by the polymer modulus. The DMA, SAXS, and DSC experiments suggest that foams made with 100% polyether polyol, 30% SAN polyol and 30% SBOP have different morphology. The compression strength improvements are achieved via different mechanisms. In 30% SAN foam, compression modulus is improved through SAN particle reinforcement; and SBOP improves foam modulus via a phase mixing morphology.

Solvent extraction study probed the network connectivity and showed secondary hydroxyls in SBOP are well reacted into the networks. On the other hand, SAN copolymer polyol is not completely bonded to the polymer phase.

References

[1] M. Szycher, Szycher's Handbook of Polyurethanes, Boca Raton, CRC press, (1999).

[2] R. Herrington and K. Hock, Flexible Polyurethane Foams, Midland, MI, Dow Chemical Co., (1997).

[3] Energy Information Administration, US Dept. of Energy -- May, (2005).

[4] Z. Petrovic, I. Javni, A. Guo and W. Zhang, US Patent 6,433,121, (2002).

[5] Z. Lysenko, D. L. Morrison, D. A. Babb, D. L. Bunning, C. W. Derstine, J. H. Gilchrist, R. H. Jouett, J. S. Kanel, K. D. Olson, W. J. Peng, J. D. Phillips, B. M. Roesch, A. W. Sanders, A. K. Schrock and P. J. Thomas, WO Patent 096744, (2004).

[6] B. F. Schaefer, *Science*, **308**, 1267, (2005).

[7] Z. S. Petrovic, W. Zhang and I. Javni, *Biomacromolecules*, **6**, 713, (2005).

[8] R. Herrington and J. Malsam, US Patent Publication 0070620, (2005).

[9] X. Han, C. Zeng, J. L. Lee, K. W. Koelling and D. L. Tomasko, *Polym Eng Sci*, **43**, 1261, (2003).

[10] M. B. Rhodes and B. Khaykin, *Langmuir*, **2**, 643, (1986).

[11] B. D. Kaushiva, D. V. Dounis and G. L. Wilkes, *J Appl Polym Sci*, **78**, 766, (2000).

[12] E. A. Blair, *ASTM-STP 414*, 84, (1967).

[13] F. A. Shutov, Cellular Structure and Properties of Foamed Polymers, Munich, Hanser, (1991).

[14] L. J. Gibson and M. F. Ashby, *Proc. R. Soc. Lond. A*, **382**, 43, (1982).

[15] C. Kau, L. Huber, A. Hiltner and E. Baer, *J Appl Polym Sci*, **44**, 2081, (1992).

[16] B. Niederoest, C. Y. Chan and N. C. Silverman, US Patent 6,716,890, (2004).

[17] R. F. Harris, M. D. Joseph, C. Davidson, C. D. Deporter and V. A. Dais, *J Appl Polym Sci*, **41**, 509, (1990).

[18] J. W. Rosthauser, K. W. Haider, C. Steinlein and C. D. Eisenbach, *J Appl Polym Sci*, **64**, 957, (1997).

[19] S. L. Cooper and A. V. Tobolsky, *J Appl Polym Sci*, **11**, 1361, (1967).

[20] Z. S. Petrovic, I. Javni and G. Banhegy, *Journal of Polymer Sciece: Part B: Polymer Physics*, **36**, 237, (1998).

[21] R. Neff, A. Adedeji, C. W. Macosko and A. J. Ryan, *J Polym Sci B: Polym Phys*, **96**, 579, (1998).

Keywords

Polyurethane flexible foam, Soybean oil polyol, and morphology.